P13.203 CASE STUDIES OF WINTER PRECIPITATION EVENTS USING 2D-VIDEO DISDROMETERS AND C-BAND RADAR

Gwo-Jong Huang[1], V. N. Bringi[1], W.A. Petersen[2], L. Carey[3], C.J. Schultz[3] and P.N. Gatlin[3]

[1] Department of Electrical and Computer Engineering, Colorado State University, Fort Collins, Colorado
[2] NASA/Wallops Flight Facility, Wallops Island, Virginia
[3] University of Alabama, Huntsville, Alabama

1. INTRODUCTION

Winter precipitation can consist of a large variety of particle types including pristine crystals, aggregates of crystals (or snow), rimed snow, and graupel to name a few. Of interest to remote sensing by radar or radiometers are the particle "size" distributions (PSD), the density versus "size" relationship and particle models used to compute the scattering and extinction cross-sections at various frequencies. Note that "size" is in quotes here as there is no commonly accepted definition of "size" (also referred to as characteristic length). Once the aforementioned attributes are known one can compute relevant parameters of practical importance such as liquid equivalent snow rate (LESR or simply SR), or the liquid equivalent snow accumulation: LESA or simply SA), or the equivalent radar reflectivity factor (Z_e) from which the ubiquitous power laws of the form $Z_e=a(SR)^b$ can be estimated. In a previous article by Huang et al. (2010), a methodology was developed to use data from a 2D-video disdrometer (2DVD) and C-band radar to arrive at Z_e-SR relations for 7 winter precipitation events.

The NSSTC site in Huntsville, AL has a number of 2DVDs (SN25, SN37 and SN38) located close to each other (several m) along with other instrumentation under the umbrella coverage of the ARMOR C-band dual-polarized radar. All three units are the newer, compact design. One winter precipitation event is analyzed here (event of 10 Jan 2011) from the viewpoint of (i) instrument-to-instrument variability of some parameters such as Z_e and SR, (ii) using fall speed and PSD data from the 2DVDs along with the theory of Böhm (1989) to estimate the density versus "size" power law, and (iii) to compare the 2DVD-based estimates of liquid equivalent snow accumulation (SA) with a Geonor weighing gauge. We also have similarly analyzed one winter event from the Helsinki area where 2DVD and other data were available under the auspices of the Light Precipitation Validation Experiment (LPVEx). The event of 30 Dec 2010 occurred at much colder temperatures than the Huntsville event and we expect the microphysics to be quite different also. For the event from LPVEx, we have compared the snow accumulation from 2DVD with an OTT Pluvio weighing precipitation gauge (exactly the same procedures were used for both the Huntsville and Helsinki events). In addition, the 2DVD-derived Z_e-SR relation for the Helsinki event was used to derive a radar-based snow accumulation map.

2. THE 2DVD DISDROMETER

The 2DVD is described in detail by Schönhuber et al. (2008), and a schematic is given in Fig. 1. Earlier work related to using the 2DVD for snow particles are, for example, Schönhuber et al. (2000), Hanesch (1999) and Brandes et al. (2007). The instrument computes the particle fall speed and gives two orthogonal images of the particle using high speed line scan cameras. Fig. 2 shows an example of a snow particle image from the two cameras.

Corresponding author address: Gwo-Jong Huang, Dept. of Electrical and Computer Engineering, Colorado State University, Fort Collins, CO 80523-1373

E-mail: gh222106@engr.colostate.edu

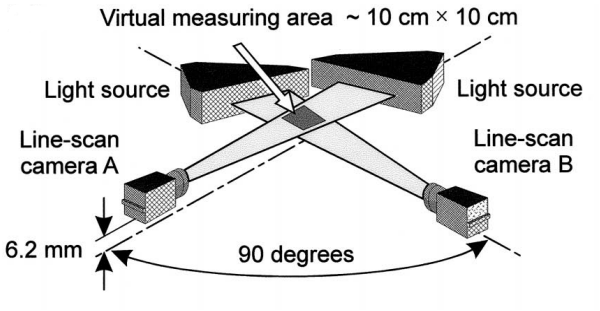

Fig. 1: Schematic showing the geometry of the 2DVD. From Kruger and Krajewski (2002). For details of the instrument please refer to Schönhuber et al. (2008).

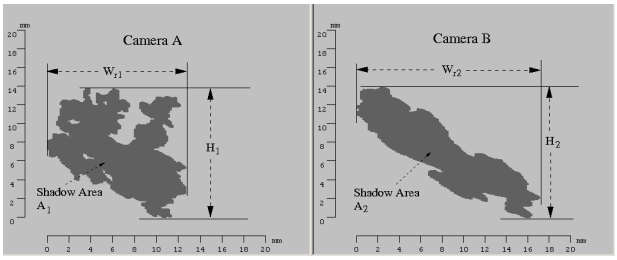

Fig. 2: Front and side view images of a snow flake from the 2DVD. The maximum "size" is approximately 16 mm in the side view (Camera B). From Huang et al. (2010).

Note that the true volume of the snow particle cannot be determined from such imaging instruments. For each (orthogonal) view as illustrated in Fig. 2 we have the following: the height H (which should be very close in value), the width W and the area (A) of the 'shadowed' pixels.

The 'apparent' volume from the 2 views is calculated as:

$$V_{app} = \frac{\pi}{6} D_{app}^3$$

$$= \frac{\pi}{6}\left(W_1 \cdot W_2 \cdot H\right)$$

where H is the geometric mean of (H_1,H_2), and

$$W_{1,2} = \frac{4A_{e1,e2}}{\pi \cdot H}$$

Note that A_{e1} and A_{e2} are the shadowed areas.

The widths $W_{1,2}$ are calculated assuming the shadowed area equals the area of an equivalent ellipse with widths of $W_{1,2}$ (major axis of ellipse) and height H (minor axis of ellipse) ,respectively. The D_{app} is the equi-volume spherical diameter where the volume is V_{app}. The particle size distribution is obtained from the set of all matched particles (detected within the virtual measuring area in Fig. 1) and denoted by $N(D_{app})$. The matching procedure is described in Huang et al. (2010): however, the matching criteria results in some fraction of the total number of particles being rejected which underestimates the concentration. To adjust $N(D_{app})$ for this underestimate (assumed to be a constant factor γ) the following procedure is used. According to Schönhuber et al. (2008), the active area for a single camera is 250 cm^2. Assuming that the particles are falling uniformly within the entire active area, the ratio of total number of particles counted within the virtual measuring area to the total number within the active area will be under ideal conditions equal to 100/250=0.4. So to adjust (scale) the $N(D_{app})$ due to rejected particles, a factor γ is used which forces the actual ratio to 0.4. In practice, γ is computed from both cameras and averaged.

3. BÖHM's METHOD

Here, we use the theory of Böhm (1989), who developed a general equation for the terminal fall speed of solid hydrometeors, and the approach of Hanesch (1999) who used 2D-video disdrometer (2DVD) data to determine the fall speed versus mass relation. Böhm's formula for the terminal fall speed depends on three parameters, (i) mass, (ii) the mean circumscribed area (A) presented to the flow and (iii) the mean effective projected area (A_e) presented to the flow (see Fig. 3). It includes environmental conditions such as air density, viscosity and temperature. For our purposes, the 2DVD (see Fig. 1) measures the fall speed of each particle, and the A and A_e can be estimated from knowledge of the shadowed pixels from each camera view (see Fig. 2). The circumscribed ellipse area A_1 is approximately defined by the axes dimensions W_{r1} (maximum width) and H_1 (similarly for Camera B it is A_2). In order to use Böhm's approach we assume that the shadowed area from the 2DVD (front and side views) is expected to be similar to the bottom view (which is presented to the flow). This assumption is likely not valid for pristine crystals (e.g., plates, needles, dendrites).

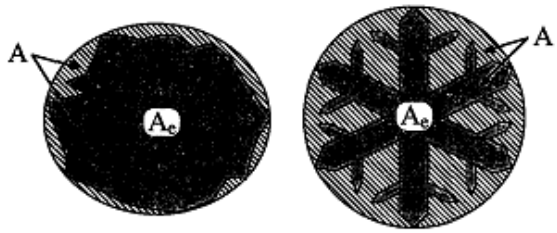

Fig 3: Definition of cross sectional areas A_e (the shadowed area), and A (the minimum circumscribed area). From Böhm (1989).

Böhm's method was developed to give a simple formula for the terminal fall speed in terms of mass and (A/A_e) (with additional air density and viscosity). Here we use the fall speed from the 2DVD to compute the mass of each particle (from equations 8,10,11 given in Böhm 1989). From the mass and D_{app}, we estimate the particle's apparent density (ρ). For all particles within a time window during the precipitation event, we fit a power law of the form $\rho=\alpha D_{app}^{\beta}$. The liquid equivalent snow rate (SR) is then computed as:

$$SR = \frac{1}{A\,\Delta t}\sum_{n}\rho(D_{app})\,V_{app,n}$$

where A is the virtual measuring area and Δt is the integration time. The Z_e is computed using the T-matrix method using $N(D_{app})$ and ρ, and assuming oblate spheroidal shape with axis ratio=0.8 and Gaussian canting angle distribution with [0°, σ=40°] (nearly random orientation).

4. INSTRUMENT-TO-INSTRUMENT COMPARISON

Since we had two identical 2DVDs (compact design) located side-by-side, it was possible to calculate the instrument errors (mainly due to finite sampling area and possible matching errors) for some variables such as SR and Z_e. As an example we have chosen the 10 Jan 2011 precipitation event in Huntsville. Fig. 4-5 show the scatter plot of SR and Z_e from the two instruments. Here we assume the $\rho(D_{app})$ from Brandes et al. (2007). The precise form for the latter is not important for these comparisons.

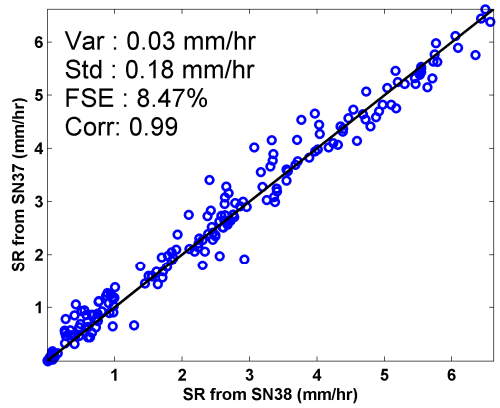

Fig. 4: Scatter plot of liquid equivalent snow rate (SR) from two identical 2DVDs (SN37 and 38).

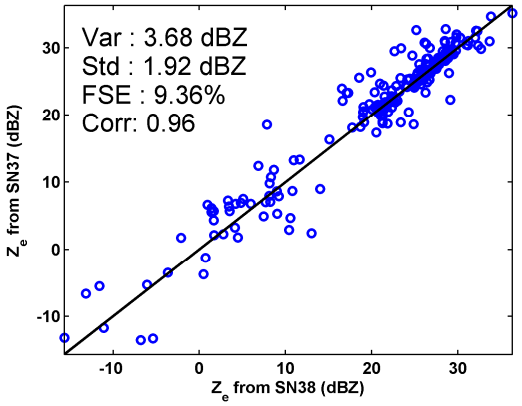

Fig. 5: As in Fig. 4 except equivalent reflectivity factor (Z_e).

In each of Fig.4-5, the statistics "Var" is calculated as Var(Δ)/2 where Δ is the difference between SN37 and SN38 for each variable. The fractional standard error (FSE) equals Std/mean. The instrument sampling error (or FSE: mainly due to finite sample area) is estimated as 8.47% for SR and 9.36% for Z_e. These values are very comparable to Cao et al. (2008) who obtained the FSE for two 2DVDs side-by-side as 9% for the 3rd moment and 10.25% for the 4th moment (in rain). In our case the SR is related to the 3rd moment, and Z_e to approximately the 4th moment for snow assuming density falls off as $1/D_{app}$.

5. THE HUNTSVILLE WINTER EVENT

On 10 Jan 2011, large snow event occurred in Central Alabama with highly variable snow types occurring (including thundersnow). Fig. 6 shows a WSR-88D image of Z_e at 10:00 pm EST: note

the cellular structure with embedded cells within a larger more uniform domain covering several states. The location of Huntsville is marked. Both the complex microphysics and amount of snow observed on 10 January in Huntsville were the result of an upper level disturbance coupled to a surface low pressure system transiting the Gulf of Mexico. As the surface low pressure system moved eastward and south of the Gulf States, a warm-moist plume of air overran a cold surface layer of air already resident in N. Alabama and the Tennessee Valley. Combined with the lower-mid level wind shear, bands of conditional symmetric instability formed, which resulted in the creation of heavy snow bands and occasional areas of embedded thundersnow, sleet, and more heavily-rimed snow particles.

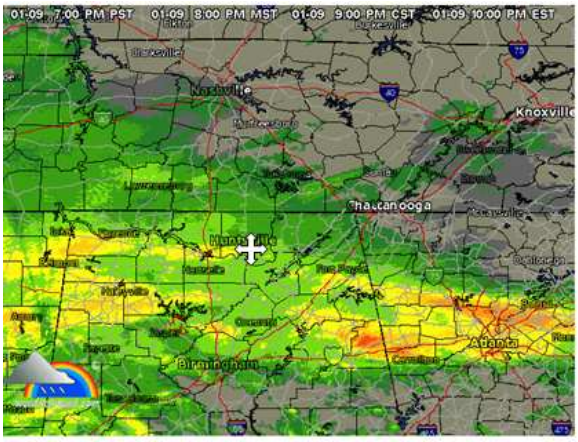

Fig. 6: Image of Z_e from WSR-88D on 10 Jan 2011. The location of Huntsville is marked with white symbol.

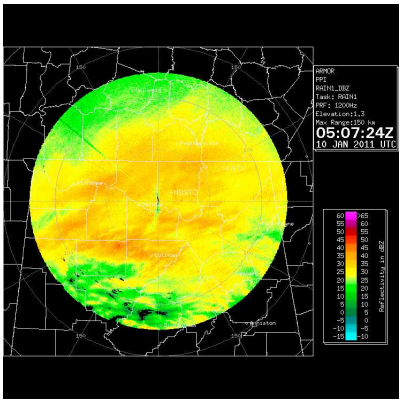

Fig. 7: PPI sweep of Z_e from ARMOR radar.

Fig. 7 shows the PPI sweep (at 05:07 UTC) at low elevation angle from the ARMOR radar which is located about 15 km SW of the 2DVD instrumented site. At this time the reflectivity appears fairly uniform with maximum values of around 35 dBZ with local maxima of 40-45 dBZ about 50 km to the SW of the radar. The Northern Alabama Lightning Mapping Array (LMA) detected at least two lightning flashes that produced intracloud VHF sources in the general vicinity of this enhanced band of reflectivity approximately 15-30 minutes prior to the PPI shown in Fig. 7 (see Schultz et al. 2011 paper this conference).

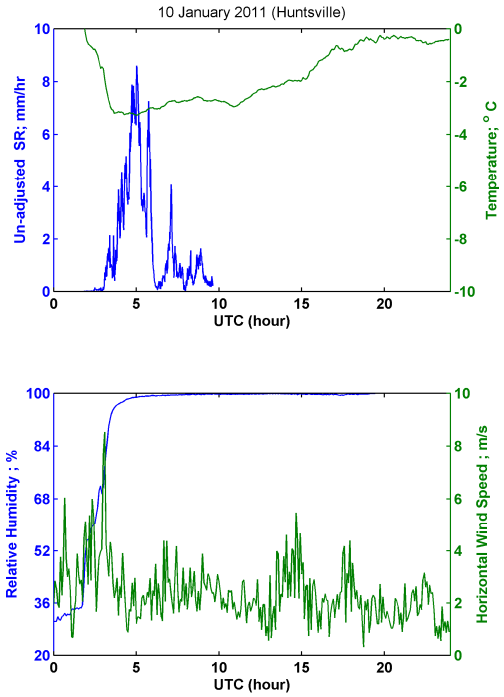

Fig. 8: Time variation of un-adjusted SR from 2DVD and other environmental parameters.

Fig. 8 shows the time variation of SR from 2DVD (un-adjusted for the γ-factor) as well as several environmental parameters. Based on these profiles we split the time interval into two periods, (i) 0-03:30 and (ii) 03:30-05:53 UTC (SN38 unit stopped operating at 05:53). For SN37 the end time was close to 09:00 UTC. In these two periods we applied Böhm's method (Section 3) to compute the $\rho(D_{app})$ power law (included in Böhm's method are viscosity and air density which are functions of temperature, relative humidity and pressure). Table 1 gives the coefficient (α) and exponent (β) of $\rho=\alpha D_{app}^{\beta}$ for the two time periods and for the two 2DVD

units (SN37 and SN38). Also given are the γ-factors.

Table 1: The γ, α and β for 10 Jan. 2011 at Huntsville.

Unit	Time	γ	α	β
SN37	00:00 - 03:30	1.16	0.20129	-0.5637
	03:30 -05:53	1	0.15861	-0.6479
SN38	00:00 – 03:30	1.24	0.19618	-0.5332
	03:30 – 05:53	1	0.16335	-0.7104

Note that for a given time interval, there is not much difference in the parameters between the two units. However, there is more difference in the parameters from the first time interval to the second interval, perhaps reflecting the change in temperature and relative humidity between these two time windows. It was noted by one of the authors (WP) that the precipitation character did appear to change with time (starting as a mixture of sleet, rimed aggregates (some graupel) and wet-snow, evolving by 0330 UTC to heavier and more dry aggregated snow composed of a wider variety of branched, and occasional columnar habits. One point that may be noted is that the value of the exponent β is quite large (-0.5 to -0.7) compared to the generally accepted value of ≈ -1 (as summarized in Brandes et al. 2007). This implies that for a given D_{app}> 1 mm, the density would be larger if β is around -0.5 to -0.7 as compared with -1. The α values (0.1-0.2) are generally in the range summarized by Brandes et al. (2007).

Fig. 9 compares the liquid equivalent snow accumulation from the Geonor gauge and from the two 2DVD units (we did not use SN25 as there was a calibration problem). The agreement is excellent with accumulation error < 10%. The peak snow rate near 05:00 UTC is well captured by the 2DVDs and the Geonor gauge.

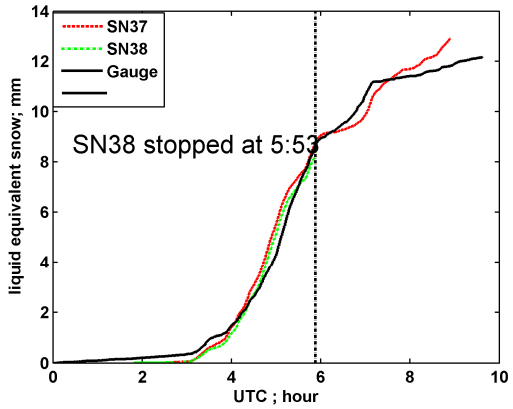

Fig. 9: Liquid equivalent snow accumulation from 2DVD units (SN37 and 38) compared with Geonor gauge for 10 Jan 2011 snow event.

6. HELSINKI EVENT OF 30 DEC 2010

The Light Precipitation Validation Experiment (LPVEx) was conducted near the Helsinki area during the Fall of 2010. We consider one precipitation event from 30 Dec 2010. While there were three instrumented sites for LPVEx, the site at Järvenpää is chosen here since it also had a vertically pointing C-band radar, but of principal interest here is the compact 2DVD unit and a OTT Pluvio gauge. We use the same procedure as described in Section 3 to compare snow accumulations derived from the 2DVD with the Pluvio gauge, and in addition we derive a Z_e-SR power law relation. This relation was applied to C-band radar measurements (from the Kumpula radar: Dmitri Moisseev, personal communication) to generate a radar-based snow accumulation map.

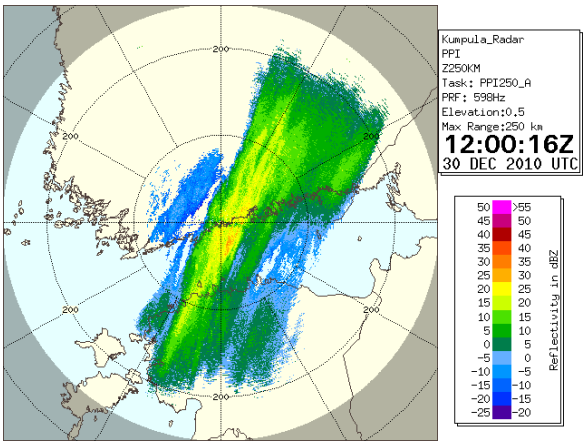

Fig. 10: PPI of Z_e from the Kumpula C-band radar. The Järvenpää site is 32 km to the NE.

Fig.10 shows a low elevation angle (0.5°) PPI sweep from the Kumpula radar at 12:00 UTC which was near the time of maximum snow rate at the Järvenpää site.

Fig. 11 shows the time variation of SR from 2DVD (un-adjusted for the γ-factor) as well as several environmental parameters for the 30 Dec 2010 event. The temperature was much colder (-10 to -8 C) as compared to Fig. 8. From the environment profiles there appeared to be no need to split the time interval for this event into sections. The application of Böhm's method applied for the entire event gave the γ-factor, and coefficient (α) and exponent (β) of $\rho=\alpha D_{app}^{\beta}$ as in Table 2.

Table 2: Same as Table 1 except for LPVEx case.

Date	Time	γ	α	β
30 Dec.	00:00–23:59	2.07	0.15133	-0.9238

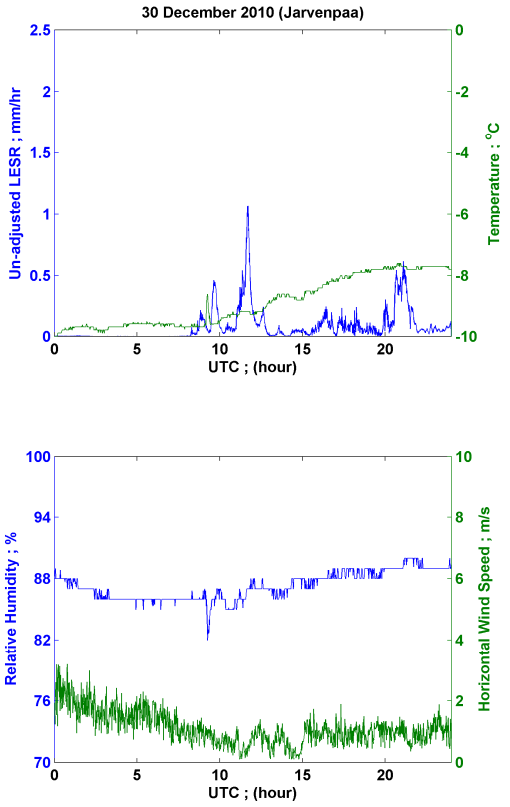

Fig. 11: Time variation of un-adjusted SR from 2DVD and other environmental parameters for the 30 Dec 2010 event.

Note that the γ-factor is much higher for the 30 Dec. event than for the Huntsville event (at Järvenpää site, the 2DVD unit was located on the roof of a building without any wind shields and hence we had limited events with low wind speeds < 3 m/s). The (α,β) values are close to that obtained by Brandes et al (2007) (0.178, -0.92); the latter values being an average of a number of winter events in Colorado. Fig. 12 shows the liquid equivalent snow accumulation from 2DVD and the Pluvio gauge. The agreement is excellent, within 10% for total accumulation (similar to Fig. 9 results).

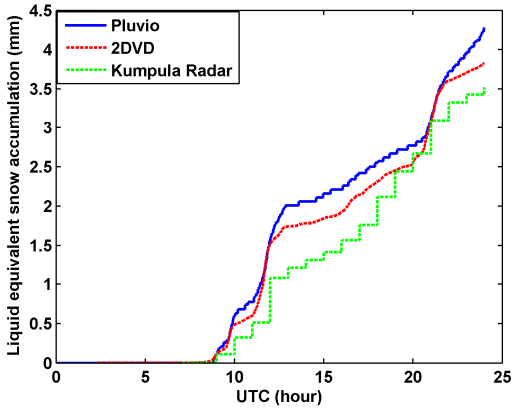

Fig. 12: Liquid equivalent snow accumulation from 2DVD compared with Geonor gauge for 30 Dec 2010 snow event. The Kumpula radar-based accumulation using the Z_e-SR fit in Fig. 13 is also shown (in green).

For this event we computed a Z_e-SR relation with Z_e computed as described towards the end of Section 3. Each data point in Fig. 13 is obtained using 1-min time averaged particle size distributions and the power law fit is also shown. There appears to be substantial scatter in the data, i.e., for a given SR the Z_e could vary by 10 dB (recall that the instrument sampling error is only 10%, see Fig. 5). Yet there is a good correlation between Z_e and SR and the fit seems reasonable and in the range given in Table 4 of Huang et al. (2010). Fig.12 also shows the Kumpula radar-based accumulation over the Järvenpää site showing good agreement.

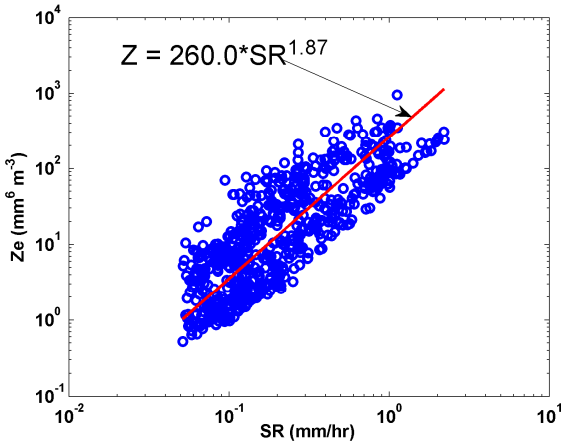

Fig. 13: Scatter plot of Z_e versus liquid equivalent snow rate (SR) obtained from 2DVD data for 30 Dec 2010 event.

A radar-based snow accumulation map for this event was made using the fit in Fig. 13 with radar Z_e measured by the Kumpula radar (see Fig. 14).

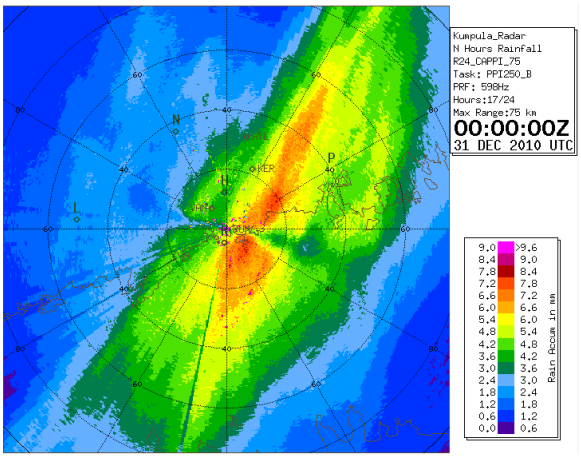

Fig. 14: C-band Kumpula radar-based snow accumulation map prepared by Dmitri Moisseev of the University of Helsinki using the Z_e-SR power law in Fig. 13. The Järvenpää site is denoted as "HYL".

The lack of any significant systematic bias for total accumulation indicates that the radar was well-calibrated. The peak accumulation from Fig. 14 (around 7-8 mm) occurred to the east of the Järvenpää site. It was possible to compare the total accumulations with 5 FMI AWS stations located < 60 km from the radar. Fig. 15 shows a scatter plot of total accumulations between the Kumpula radar-based values and the FMI AWS stations.

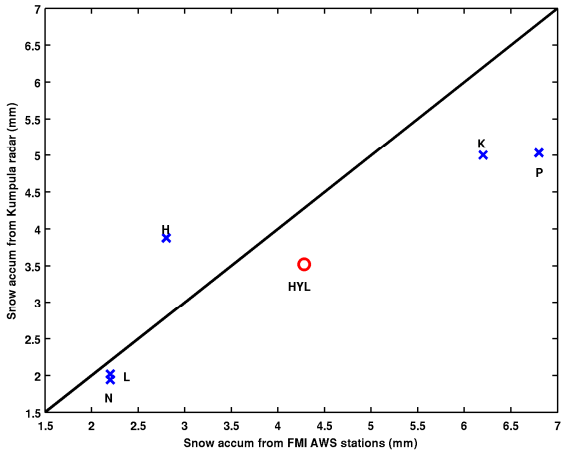

Fig. 15: Snow accumulation from Kumpula radar (using Z_e-SR relation from Fig. 13) versus 5 FMI AWS stations (marked as "x"). The open circle ("o") is the Järvenpää (HYL) site. The locations of the FMI AWS stations are in the Fig. 14.

The overall agreement and correlation is quite good considering that the Z_e-SR relation was developed from only the Järvenpää site and may not be representative under the entire radar umbrella.

7. CONCLUSIONS

The theory of Böhm (1989) was applied to 2D-video disdrometer (2DVD) data to estimate the coefficient and exponent of the density (ρ) versus apparent diameter (D_{app}) relationship in two very diverse winter precipitation events, one from Huntsville, AL and one from Helsinki. From the particle size distribution, $N(D_{app})$, the liquid equivalent snow rate and the radar reflectivity were computed. A simple method to adjust the $N(D_{app})$ due to particles being rejected by the matching procedure criteria is described. The 2DVD-based snow accumulation for the two events were compared with weighing gauges with excellent agreement (total accumulation errors<10 %). For the Helsinki event, a Z_e-SR power law was derived from the 2DVD data, and used to generate a radar-based snow accumulation map (C-band Kumpula radar). The radar-based accumulation at the location of the 2DVD site is also shown to be in excellent agreement with the weighing gauge for the Helsinki event. In addition, the radar-based accumulations were compared with 5 FMI AWS stations with good agreement. It is recommended that in the future, the 2DVD units

be located within a double fence international reference (DFIR) type wind-shield.

Acknowledgements: GJH and VNB were supported by NASA PMM science grants NNX10AJ11G and filed support grant NNX10A132G. WAP acknowledges support from the NASA PMM Program and GPM Project Office. The authors are grateful to Dmitri Moisseev of the University of Helsinki for providing data as well as generating Fig. 14.

REFERENCES

Böhm, H.P., 1989: A general equation for the terminal fall speed of solid hydrometeors., *J. Atmos. Sci.*, **46**, 2419-2427.

Brandes, E.A., K. Ikeda, G. Zhang, M. Schönhuber and R.M. Rasmussen, 2007: A statistical and physical description of hydrometeor distributions in Colorado snowstorms using a video disdrometer., *J. Appl. Meteor. and Climat.*, **46**, 634-650.

Cao, Q., G. Zhang, E. Brandes, T. Schuur, A. Ryzhkov and K. Ikeda, 2008: Analysis of Video Disdrometer and Polarimetric Radar Data to Characterize Rain Microphysics in Oklahoma., *J. Appl. Meteor. and Climat.*, **47**, 2238-2255.

Hanesch, M., 1999: *Fall velocity and shape of snowflake.*, Ph. D dissertation, Swiss Federal Institute of Technology. [Available online at http://www.distrometer.at/newReferences.html]

Huang, G., V. N. Bringi, R. Cifelli, D. Hudak and W. A. Petersen, 2010: A Methodology to Derive Radar Reflectivity–Liquid Equivalent Snow Rate Relations Using C-Band Radar and a 2D Video Disdrometer., *J. Atmos. Ocean Tech.*, **27**, 1802-1821.

Kruger, A., and W.F. Krajewski, 2002: Two-dimensional video disdrometer: A description, *J. Atmos. Oceanic Technol.*, **19**, 602-617.

Schönhuber, M., H. E. Urban, W. L. Randeu and J. P. V. Poiares Baptista, 2000: Empirical Relationships between Shape, Water Content and Fall Velocity of Snowflakes, *ESA SP-444 Proceedings*, Millennium Conference on Antennas & Propagation, April 9-14, 2000, Davos, Switzerland.

Schönhuber, M., G. Lammer and W. L. Randeu, 2008: *Precipitation: Advances in Measurement, Estimation and Prediction,* Springer, New York, 3-31.

Schultz, C.J., W.A. Petersen, L.D. Carey and E.C. Bruning: C-band dual-polarimetric observations of snowfall in a southeastern thundersnow event (P13.209, these conf. proc.)